Thiophosphoryl Complexes of Bis(cyclopentadienyl)titanium. 1. Syntheses, Interconversions, and Structures

Gregg A. Zank and Thomas B. Rauchfuss*[1]

School of Chemical Sciences, University of Illinois, Urbana, Illinois 61801

Received January 23, 1984

The reaction of $(MeCp)_2Ti(CO)_2$ (MeCp = η^5-$CH_3C_5H_4$) with perthiophosphinic acid anhydrides, $R_2P_2S_4$, gives compounds of the formula $(MeCp)_2TiS_4P_2R_2$ (R = 4-$C_6H_4OCH_3$ (An), **2a**; R = 4-$C_6H_4OC_2H_5$ (Pn), **2c**) or $(MeCp)_2TiS_3PR$ (R = *t*-Bu, **3b**; R = 3-cyclohexenyl, **3c**). The $TiS_4P_2R_2$ compounds could also be prepared from $LiBHEt_3$-reduced $R_2P_2S_4$ and $(MeCp)_2TiCl_2$ (or Cp_2TiCl_2). Spectroscopic studies indicate that the type **2** compounds contain $\overline{TiSPPS}$ rings. The reaction of Li_2S with $R_2P_2S_4$ gives Li_2S_3PR that was isolated in the case where R = An, **4**. S_3PR^{2-} reacted with $(MeCp)_2TiCl_2$ to give the aforementioned $(MeCp)_2TiS_3PR$ compounds in addition to **3a** where R = An. ^{31}P NMR studies suggest that **2a** and **3a** are in facile equilibrium (K_{eq} = 0.22), consistent with this **3a** was found to react with $[PhPS]_3$ yielding a 1:2:1 mixture of the Ph_2, AnPh, and An_2 derivatives of the TiS_4P_2 compounds. Compound **3a** reacts with $NiCl_2(Ph_2PC_2H_4PPh_2)$ faster than does **2a** giving $(MeCp)_2TiCl_2$ and $Ni(S_3PAn)(Ph_2PC_2H_4PPh_2)$. A single-crystal X-ray diffraction study confirmed that **3a** contains a $\overline{TiSPS}$ ring. **3a** crystallizes in the space group $P2_1/c$ with a = 7.304 (2) Å, b = 13.716 (3) Å, c = 23.995 (6) Å, and β = 111.28 (2)°. The structural parameters of **3a** are compared with $(Me_5C_5)_2TiS_3$ and $Me_2P_2S_4$.

Introduction

It is widely appreciated that the reactivity of non-metal fragments is substantially modified upon coordination to transition metals. In certain cases such as the S_2 moiety in $[Ir(S_2)(PR_3)_4]^+$, the reactivity of the non-metal fragment is moderated relative to the uncoordinated species.[2,3] Studies in this laboratory, however, have shown that the chalcogen-based reactivity in Cp_2TiE_5 (Cp = η^5-C_5H_5; E = S, Se) is considerably enhanced relative to the *cyclo*-E_8 analogues.[4,5] We have now extended this methodology to the study of how a Cp_2Ti moiety modifies the reactivity of a synthetically important class of P–S heterocycles.

There has been considerable recent interest in the organoperthiophosphinic acid anhydride dimers, $R_2P_2S_4$, especially where R = 4-$CH_3OC_6H_4$ (An), **1a**.[6,7] This com-

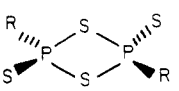

1

pound is prepared from the direct reaction of P_4S_{10} and anisole[6,8] and has proven to be a useful reagent for the thiation of organic carbonyls (eq 1).[9–11] Little is known

$$RC(=O)R' \xrightarrow{An_2P_2S_4} RC(=S)R' \qquad (1)$$

about the mechanism of this thiation reaction[12] although it is clear that the driving force derives from the considerable oxophilicity of phosphorus.[13] Furthermore, it is claimed that solutions of **1a** consist of several species.[7]

The preparation of organotitanium derivatives of **1a** could not only provide unique opportunities for some unusual synthesis but also contribute to the understanding of the chemistry of this important reagent. This present work is concerned only with the interconversion chemistry of the Cp_2Ti derivatives of **1**. A future report will elaborate upon the reactivity of these species toward various substrates.

Experimental Section

Materials and Methods. All preparative reactions and isolations were performed under an atmosphere of purified nitrogen unless otherwise noted. Tetrahydrofuran (THF), toluene, benzene, and hexanes were obtained as reagent grade solvents and redistilled from sodium benzophenone ketyl under nitrogen. Dichloromethane was redistilled from P_4O_{10}, and NMR solvents were stored under nitrogen over 4 Å molecular sieves. The anisyl-, phenetyl-, and cyclohexenylperthiophosphinic acid anhydride dimers, $R_2P_2S_4$, were prepared from the reaction of anisole (An) (**1a**), phenetole (Pn) (**1d**), or cyclohexene (Che) (**1c**) and P_4S_{10}.[8,14] The *tert*-butylperthiophosphinic acid anhydride dimer, *t*-$Bu_2P_2S_4$[15a,b] (**1b**), was prepared from *t*-$BuPCl_2$ and Li_2S_2 in a manner similar to that described by Cordes et al.[15a] One molar THF solutions of $LiHBEt_3$ were purchased from Aldrich Chemical Co. All other chemicals used in this work were commercially available or were prepared by well-established methods.

NMR measurements were made in a Nicolet NT 360 (^1H and ^{13}C NMR) and a Varian XL-100 with internal ^2H frequency lock (^{31}P NMR). Field desorption (FD) mass spectra were measured by Mr. Carter Cook on a Varian 731 spectrometer at the University of Illinois mass spectrometry laboratory.

All new compounds were isolated as crystalline solids which gave satisfactory analyses (Table I). These data were obtained

(1) Alfred P. Sloan Fellow 1983–1985. Camille and Henry Dreyfus Teacher Scholar 1983–1988.

(2) Ginsberg, A. P.; Lindsell, W. E.; Sprinkle, C. R.; West, K. W.; Cohen, R. L. *Inorg. Chem.* **1982**, *21*, 3666–81 and references therein.
(3) Hoots, J. E.; Rauchfuss, T. B. *Inorg. Chem.* **1983**, *22*, 2806–12.
(4) Bolinger, C. M.; Rauchfuss, T. B. *Inorg. Chem.* **1982**, *21*, 3947–54.
(5) Giolando, D. M.; Rauchfuss, T. B. *Organometallics* **1984**, *3*, 487–9.
(6) Maier, L. *Top. Phosphorus Chem.* **1978**, *10*, 129–69.
(7) Lawesson, S.-O. *ACS Symp. Ser.* **1982**, *No. 196*, 280 and references therein.
(8) Lechor, H. Z.; Greenwood, R. A.; Whitehouse, K. C.; Chao, T. H. *J. Am. Chem. Soc.* **1956**, *78*, 5018.
(9) Peterson, B. S.; Scheibye, S.; Nilsson, N. H.; Lawesson, S.-O. *Bull. Soc. Chim. Belg.* **1978**, *87*, 223–8.
(10) Peterson, B. S.; Scheibye, S.; Clausen, K.; Lawesson, S.-O. *Bull. Soc. Chim. Belg.* **1978**, *87*, 293–7.
(11) Scheibye, S.; Peterson, B. S.; Lawesson, S.-O. *Bull. Soc. Chim. Belg.* **1978**, *87*, 229–38.
(12) Rasmussen, J. B.; Jorgensen, K. A.; Lawesson, S.-O. *Bull. Soc. Chim. Belg.* **1978**, *87*, 307–8.
(13) For example see: Schrauzer, G. N.; Mayweg, V. P.; Heinrich, W. *Inorg. Chem.* **1965**, *4*, 1615.
(14) Fay, P.; Lankelma, H. P. *J. Am. Chem. Soc.* **1952**, *74*, 4933.
(15) (a) Shore, J. T.; Noble, M. C.; Cordes, A. W. "Abstracts of Papers", 184th National Meeting of American Chemical Society, Kansas City, MO, Sept 1982; American Chemical Society: Washington, DC, 1982. (b) Baudler, M.; Gruner, C.; Furstenburg, G.; G.; Kloth, B.; Saykowski, F.; Ozer, U. *Z. Anorg. Allg. Chem.* **1978**, *446*, 169–76.

0276-7333/84/2303-1191$01.50/0

Table I. Analytical Data (Theoretical Values in Parentheses)

	C	H	S	P	M
$(MeCp)_2TiS_4P_2An_2$ $C_{26}H_{28}S_4P_2O_2Ti$ **2a**	51.20 (51.15)	4.99 (4.62)	19.60 (21.01)	10.00 (10.14)	7.92 (7.84)
$Cp_2TiS_4P_2An_2$ $C_{24}H_{24}S_4P_2O_2Ti$ **2b**	49.85 (49.48)	4.34 (4.15)	20.60 (22.02)	10.07 (10.63)	8.33 (8.22)
$(MeCp)_2TiS_4P_2Pn_2$ $C_{28}H_{32}S_4P_2O_2Ti$ **2c**	52.87 (52.66)	5.26 (5.05)		9.84 (9.69)	7.34 (7.50)
$(MeCp)_2TiS_3PAn$ $C_{19}H_{21}S_3POTi$ **3a**	51.60 (51.81)	4.89 (4.81)		7.16 (7.03)	10.65 (10.88)
$(MeCp)_2TiS_3P$-*t*-Bu $C_{16}H_{23}S_3PTi$ **3b**	48.99 (49.24)	5.83 (5.94)	24.35 (24.65)	8.11 (7.94)	12.23 (12.27)
$(MeCp)_2TiS_3PChe$ $C_{18}H_{23}S_3PTi$ **3c**	52.06 (52.17)	5.68 (5.49)	23.10 (23.21)	7.63 (7.47)	11.05 (11.56)
$Li_2S_2P(S)An\cdot THF$ $C_{11}H_{15}S_3O_2PLi_2$ **4**	42.64 (42.25)	4.85 (4.72)		9.28 (9.68)	4.12 (4.33)
$NiS_3PAn(dppe)$ $C_{33}H_{31}S_3P_3ONi$ **5**	57.27 (57.33)	4.45 (4.52)		12.67 (13.44)	8.49 (8.49)
$[NiS_2P(SMe)An(dppe)]PF_6$ $C_{34}H_{34}S_3P_4ONiF_6$ **6**	48.09 (47.97)	4.04 (4.03)		14.52 (14.55)	6.92 (6.79)

by the University of Illinois microanalytical laboratory.

$(C_5H_4R)_2TiS_4P_2R_2'$ (2a, R = CH_3, R' = An; 2b, R = H, R' = An; 2c, R = CH_3, R' = Pn). Method A. In a representative reaction, a slurry of $Cp_2Ti(CO)_2$[16] (235 mg, 1 mmol) and $An_2P_2S_4$ (**1a**, 404 mg, 1 mmol) in 50 mL of THF was stirred for 1 h. After this time the dark brown solution was diluted with hexanes (40 mL) to precipitate the crude product, which was recrystallized by addition of benzene (20 mL) to a CH_2Cl_2 solution (40 mL) of the crude product followed by concentration. Subsequent filtration afforded a 76% yield (450 mg) of exceedingly air-sensitive red-purple crystals of **2b**.

Method B. To a stirred slurry of **1a** (404 mg, 1 mmol) in THF (30 mL) was added $LiHBEt_3$ as a 1 M solution in THF (2 mL, 2 mmol). Gas was evolved, and solid Cp_2TiCl_2 (250 mg, 1 mmol) was added to the pale yellow solution of reduced **1a**. After being stirred 15 min, the dark brown reaction solution was worked up in a manner identical with that described in method A; yield 71% (400 mg).

$(C_5H_4CH_3)_2TiS_3PAn$ (3a). Addition of a THF (40-mL) solution of $(MeCp)_2TiCl_2$ (2.21 g, 8 mmol) to **4** (2.56 g, 8 mmol) (vide infra) gave a dark red solution that was stirred for 1 h and evaporated. The residue was extracted with three portions (40 mL) of CH_2Cl_2, filtered through Celite, and diluted with THF (10 mL) and toluene (20 mL). The resultant solution was concentrated to $^1/_{10}$ volume and cooled to −78 °C. Subsequent filtration afforded lustrous green crystals of **3a** (2.05 g, 58%).

$(C_5H_4CH_3)_2TiS_3PR$ (3b, R = *t*-Bu; 3c, R = Che). Method A. In a representative reaction a THF (10-mL) solution of $(MeCp)_2Ti(CO)_2$ (262 mg, 1 mmol) was added to a stirred solution of *t*-$Bu_2P_2S_4$ (**1b**, 304 mg, 1 mmol) in THF (30 mL). After 20 h, toluene (10 mL) was added and the solution concentrated to ca. 15 mL and filtered to afford **3b** in 59% yield (230 mg) as dark red-brown moderately air-sensitive crystals.

Method B. To a stirred slurry of S_8 (64 mg, 0.25 mmol) in THF (10 mL) was added $LiHBEt_3$ as a 1 M solution in THF (4 mL, 4.0 mmol).[17] The resulting homogeneous pale yellow solution is added, via stainless steel cannula, dropwise to a solution of **1b** (304 mg, 1.0 mmol) in THF (10 mL). After being stirred 10 min, this Li_2S_3PR solution was added to a solution of $(MeCp)_2TiCl_2$ (554 mg, 2.0 mmol) in THF (20 mL). The resulting dark red homogeneous solution was stirred for 1 h and then evaporated. Filtration of CH_2Cl_2 extracts of the crude product through a bed of celite afforded red-brown solutions free of any inorganic salts that were diluted with toluene (15 mL), concentrated (to 10 mL), and filtered affording a 45% yield (350 mg) of dark red-brown crystals of **3b**.

Li_2S_3PAn (4). A THF (40 mL) solution of Li_2S (prepared from $LiHBEt_3$ (20 mL) and S_8 (320 mg) as described earlier) was added to **1a** (2.02 g, 5 mmol) in THF (20 mL) and stirred for 1 h. After this time addition of toluene (20 mL) followed by concentration to 20 mL and cooling to −78 °C afforded **4** in 93% yield (2.98 g) as the white crystalline THF solvate.

$NiS_3PAn(Ph_2P(CH_2)_2PPh_2)$ (5). Method A. Solid $NiCl_2$(dppe) (528 mg, 1 mmol) was added to a purple solution of **2a** (528 mg, 1 mmol) in THF (30 mL). The resulting orange solution was stirred 20 h and evaporated. The product **5** was recrystallized by dilution of its CH_2Cl_2 solutions with methanol: yield 91% (627 mg).

Method B. Addition of solvent (THF/C_6D_6, 2/1 volume to volume) to a 12-mm NMR tube containing a mixture of $NiCl_2$(dppe) (27.0 mg, 0.05 mmol) and **3a** (22 mg, 0.05 mmol) causes an immediate color change from red-brown to orange. A ^{31}P NMR spectrum of this mixture immediately after dissolution showed no resonances corresponding to **3a** or $NiCl_2$(dppe) but only those attributable to **5**.

Method C. A THF (30-mL) solution of Li_2S (2 mmol) (prepared from $LiHBEt_3$ (4 mL) and S_8 (64 mg) as previously described) was added to **1a** (404 mg, 1 mmol) and stirred for 1 h. The resulting homogeneous solution of in situ prepared **4** was added to a THF (20-mL) slurry of $NiCl_2$(dppe) (1.05 g, 2 mmol) and stirred for 2 h. Removal of the THF followed by extraction with CH_2Cl_2 (80 mL), addition of MeOH (20 ML), concentration to 30 mL, and cooling to −25 °C effected precipitation of the product. Filtration of the solution followed by washing with cold MeOH afforded an 83% yield (1.15 g) of **5** as orange crystals.

$[Ni(S_2P(SMe)An)(Ph_2P(CH_2)_2PPh_2)](PF_6)$ (6). A CH_2Cl_2 solution (30 mL) of **5** (346 mg, 0.5 mmol) and $MeSO_3F$ (82 ml, 1.0 mmol) was stirred for 4 h. After removal of the solvent and dissolution of the residue in methanol (30 mL), a methanol (10-mL) solution of NH_4PF_6 (200 mg, 1.25 mmol) was added and the resulting solution stirred 3 h. Concentration of the methanol to 5 mL, cooling to −25 °C, filtration, and washing with cold methanol yielded 385 mg (91%) of orange crystalline $[Ni(S_2(P(SMe)An))(dppe)](PF_6)$ (**6**).

X-ray Crystallography. Opaque blue-green long prismatic crystals of $(MeCp)_2TiS_3PAn$, **3a**, were obtained by slow diffusion of benzene into a concentrated THF solution of **3a** and sealed

(16) Demerseman, B.; Bouquet, G.; Bigorgne, M. *J. Organomet. Chem.* **1975**, *101*, C24–6.

(17) Gladysz, J. A.; Wong, V. K.; Jick, B. S. *Tetrahedron* **1979**, *35*, 2329–35.

Table II. A Listing of the Positional and Thermal Parameters for the Non-Hydrogen Atoms of $(CH_3C_5H_4)_2TiS_3PAn$

	X/A	Y/B	Z/C		X/A	Y/B	Z/C
Ti	0.31890 (7)	0.08126 (3)	0.21282 (2)	C8	0.3690 (5)	0.1177 (3)	0.1215 (2)
S1	0.3046 (1)	−0.08732 (5)	0.17297 (3)	C9	0.4842 (6)	0.1784 (3)	0.1669 (2)
S2	−0.0242 (1)	0.04328 (5)	0.19942 (3)	C10	0.3558 (6)	0.2388 (2)	0.1828 (2)
S3	0.0472 (1)	−0.18810 (6)	0.25313 (4)	C11	0.1652 (6)	0.2130 (2)	0.1474 (2)
P	0.0456 (1)	−0.09919 (5)	0.18850 (3)	C12	−0.0016 (8)	0.0918 (4)	0.0613 (2)
O	−0.5720 (4)	−0.2602 (2)	−0.0299 (1)	C13	−0.1348 (4)	−0.1417 (2)	0.1185 (1)
C1	0.3559 (4)	0.0724 (2)	0.3189 (1)	C14	−0.0869 (5)	−0.2088 (3)	0.0832 (2)
C2	0.4520 (4)	−0.0069 (2)	0.3053 (1)	C15	−0.2293 (5)	−0.2500 (3)	0.0334 (2)
C3	0.6076 (5)	0.0281 (3)	0.2891 (1)	C16	−0.4206 (5)	−0.2243 (2)	0.0186 (1)
C4	0.6071 (5)	0.1299 (3)	0.2927 (2)	C17	−0.4718 (5)	−0.1590 (3)	0.0541 (2)
C5	0.4468 (5)	0.1574 (2)	0.3081 (1)	C18	−0.3300 (5)	−0.1185 (3)	0.1037 (2)
C6	0.1962 (6)	0.0680 (3)	0.3440 (2)	C19	−0.5311 (8)	−0.3379 (4)	−0.0617 (2)
C7	0.1706 (5)	0.1376 (2)	0.1084 (1)				

	U(11) (U(isu))	U(22)	U(33)	U(23)	U(13)	U(12)
Ti	0.0336 (3)	0.0278 (2)	0.0359 (3)	0.0038 (2)	0.0120 (2)	−0.0004 (2)
S1	0.0365 (4)	0.0344 (3)	0.0537 (4)	−0.0035 (3)	0.0235 (3)	0.0001 (3)
S2	0.0354 (3)	0.0337 (3)	0.0477 (4)	−0.0025 (3)	0.0179 (3)	0.0036 (3)
S3	0.0524 (5)	0.0436 (4)	0.0496 (5)	0.0106 (3)	0.0205 (4)	−0.0050 (3)
P	0.0326 (3)	0.0301 (3)	0.0383 (4)	−0.0003 (3)	0.0156 (3)	−0.0008 (3)
O	0.061 (2)	0.085 (2)	0.064 (2)	−0.031 (1)	0.007 (1)	−0.011 (1)
C1	0.046 (2)	0.048 (2)	0.032 (1)	0.001 (1)	0.008 (1)	0.003 (1)
C2	0.045 (2)	0.036 (1)	0.038 (2)	0.007 (1)	0.011 (1)	0.005 (1)
C3	0.038 (2)	0.059 (2)	0.045 (2)	0.004 (2)	0.007 (1)	0.004 (1)
C4	0.049 (2)	0.055 (2)	0.051 (2)	0.008 (2)	0.001 (2)	−0.019 (2)
C5	0.064 (2)	0.038 (2)	0.044 (2)	−0.003 (1)	0.006 (2)	−0.003 (1)
C6	0.073 (3)	0.073 (3)	0.043 (2)	0.002 (2)	0.028 (2)	0.019 (2)
C7	0.055 (2)	0.041 (2)	0.035 (2)	0.008 (1)	0.016 (1)	0.002 (1)
C8	0.071 (2)	0.046 (2)	0.059 (2)	0.017 (2)	0.042 (2)	0.013 (2)
C9	0.054 (2)	0.067 (2)	0.067 (2)	0.023 (2)	0.022 (2)	−0.015 (2)
C10	0.096 (3)	0.033 (2)	0.047 (2)	0.007 (1)	0.018 (2)	−0.013 (2)
C11	0.067 (2)	0.036 (2)	0.051 (2)	0.014 (1)	0.026 (2)	0.016 (2)
C12	0.088 (3)	0.089 (3)	0.042 (2)	0.012 (2)	0.004 (2)	−0.022 (3)
C13	0.038 (1)	0.036 (1)	0.040 (2)	−0.004 (1)	0.017 (1)	−0.004 (1)
C14	0.045 (2)	0.055 (2)	0.054 (2)	−0.011 (2)	0.016 (2)	0.008 (1)
C15	0.062 (2)	0.049 (2)	0.049 (2)	−0.015 (2)	0.022 (2)	−0.001 (2)
C16	0.051 (2)	0.051 (2)	0.046 (2)	−0.009 (1)	0.014 (1)	−0.008 (1)
C17	0.037 (2)	0.092 (3)	0.091 (3)	−0.041 (2)	0.007 (2)	0.006 (2)
C18	0.043 (2)	0.080 (3)	0.070 (2)	−0.036 (2)	0.013 (2)	0.007 (2)
C19	0.092 (3)	0.071 (3)	0.055 (2)	−0.023 (2)	0.024 (2)	−0.021 (3)

in 0.5-mm capillaries under an atmosphere of purified nitrogen. Since attempts to cleave the crystals were unsuccessful, the most suitable sample was selected on the basis of precession photographs.[18] The selected sample was bound by the forms {001}, {011}, {0,1,−1}, and {100} with interfacial separations of 0.20, 0.28, 0.30, and 1.04 mm, respectively. The sample was mounted with the (1,0,−1) scattering planes roughly normal to the spindle axis. Cell parameters and intensity data were measured at ambient temperature by using Mo radiation ($\lambda(K\alpha) = 0.71069$ Å) on a Syntex $P2_1$ automated diffractometer equipped with a graphite monochromator. One unique axis along with systematic absences for $0k0$, $k = 2n + 1$, and $h0l$, $l = 2n + 1$, suggested the monoclinic space group $P2_1/c$ with parameters $a = 7.304$ (2) Å, $b = 13.716$ (3) Å, $c = 23.995$ (6) Å, $\beta = 111.28$ (2)°, $V = 224.0$ (9) Å^3, and $\rho_{calcd} = 1.421$ g cm^{-3} for $Z = 4$. The observed density, 1.35 g cm^{-3}, measured by flotation in an aqueous solution of $ZnBr_2$ was in good agreement with the calculated density. The quadrant $\pm hkl$ was collected from 2θ values of 3.0–55.0° using a $2\theta/\theta$ scanning technique with a range from 0.8° below the calculated $K\alpha_1$ peak position to 1.0° above $K\alpha_2$ position at variable scan rates from 2.0 to 19.5°/min. Of the 5283 unique intensities processed, 3365 were observed at the $2.58\sigma(I)$ level of confidence and only these reflections were used during refinement. The data were isotropically corrected for a 5% decline in the average intensity of three standards monitored for every 100 reflections and numerically corrected for absorption.

The positions for the titanium, phosphorus, and sulfur atoms of **3a** were deduced from an E map.[19] A subsequent weighted difference Fourier summation gave positions for all of the remaining non-hydrogen atoms of the complex. Following several least-squares refinement cycles, the difference Fourier map revealed a benzene solvate molecule located on the inversion center.[20] In the final cycle of least squares, the hydrogen atoms of the solvate were fixed in idealized positions (1.08 Å from respective carbon atoms) and a group isotropic thermal parameter was refined for all three. Positions for the remaining hydrogen atoms were refined with independent isotropic thermal coefficients. All non-hydrogen atoms were refined with anisotropic thermal coefficients. Successful convergence, indicated by a maximum shift/esd for the last cycle of 0.05, led to conventional residuals of $R = 0.035$ and $R_w = 0.044$.[21] The final difference Fourier map was featureless, and there were no apparent systematic errors despite the large sample size. A listing of the atomic coordinates for **3a** is given in Table II.

Results

Synthetic Studies. The reaction of $Cp_2Ti(CO)_2$ (or $(MeCp)_2Ti(CO)_2$) (Cp = η^5-C_5H_5; MeCp = η^5-$CH_3C_5H_4$) with THF slurries of $An_2P_2S_4$, **1a** (or $Pn_2P_2S_4$, **1d**), afforded

(18) Crystals of **3a** decomposed rapidly, owing to its air sensitivity and perhaps the loss of the benzene solvate molecules, and seemed invariably too fragile to cleave without enhancing the rate of this decomposition. The morphology of the selected sample was less than ideal, but the selection was limited.

(19) The structure was solved by MULTAN 80, a system of computer programs for the automatic solution of crystal structures from X-ray diffraction data, 1980: Main, P.; Fiske, S. J.; Hull, S. E.; Lessinger, L.; Germain, G.; Declercq, J.-P.; Woolfson, M. M. All other calculations were performed by SHELX 76, a program for crystal structure determination, University of Cambridge, United Kingdom, 1976, Sheldrick, G. M.

(20) Solvate coordinates (X/A, Y/B, X/C) of (0.1432 (7), −0.0469 (5), 0.5441 (3)); (0.0778 (9), −0.0821 (4), 0.4866 (3)); (−0.0647 (9), −0.0335 (5), 0.4435 (2)).

(21) The function minimized was $\sum w(|F_o| - |F_c|)^2$ where $R = \sum||F_o| - |F_c||/\sum|F_o|$, $R_w = [\sum w(|F_o| - |F_c|)^2/\sum w(|F_o|)^2]^{1/2}$, and $w = 1/\sigma(F)^2$. The estimated error in a reflection with unit weight was 1.55, where $E = [\sum w(|F_o| - |F_c|)^2/(NO - NV)]^{1/2}$.

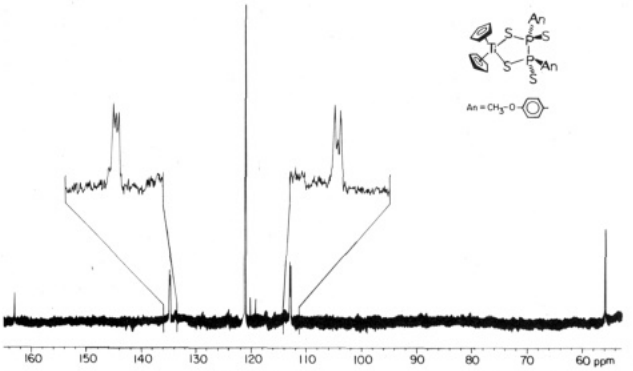

Figure 1. 90.5-MHz $^{13}C\{^1H\}$ NMR spectrum of $Cp_2TiS_4P_2An_2$ (**2b**) in CD_2Cl_2.

high yields of red-purple crystalline $(C_5H_4R)_2TiS_4P_2R'_2$ (R = CH_3, R′ = An; R = H, R′ = An; R = CH_3, R′ = Pn, **2a–c**, respectively). The same compounds can be prepared from Cp_2TiCl_2 and $LiHBEt_3$-reduced **1a(d)**. Compounds **2a–c** were characterized by microanalysis (Table I), NMR, and field desorption mass spectrometry (FDMS) (Table III). ^{31}P NMR spectroscopy of **2a–c** revealed that the phosphorus atoms were equivalent, although samples of **2a** invariably exhibited a small resonance at 33 ppm that was initially attributed to an impurity. The ^1H NMR spectra of **2a–c** established the presence of the equivalent pairs of both cyclopentadienyl and aromatic groups. The ^{13}C NMR spectrum of **2b** reaffirmed these results and provided additional structural information in that the ortho and meta carbon resonances of the anisole groups appeared as "filled in doublets" characteristic of virtual coupling arising from $|J_{PP'}| \approx 7$ Hz (Figure 1).[22] This observation suggests that the phosphorus atoms are linked while the lack of any discernible ^{31}P coupling to the ^1H of ^{13}C cyclopentadienyl resonances suggested the absence of any Ti–P bonds. Taken collectively these spectroscopic data indicate that compounds **2a–c** have a structure consisting of a $\overline{\text{TiSPPS}}$ ring (eq 2).

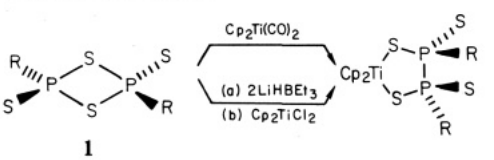

(2)

R = An, Pn

The reaction of $(MeCp)_2Ti(CO)_2$ with the alkyl phosphorus(V) compounds t-$Bu_2P_2S_4$, **1b**, or $Che_2P_2S_4$, **1c** (Che = 3-cyclohexenyl), is a markedly slower reaction than that found for **1a** or **1d** despite the high solubility of these alkyl derivatives. Reaction of **1b** or **1c** and $(MeCp)_2Ti(CO)_2$ gave good yields of $(MeCp)_2TiS_3PR$, **3b** (R = t-Bu) and **3c** (R = Che) (Table I). The formation of **3b** and **3c** from $R_2P_2S_4$ and $(MeCp)_2Ti(CO)_2$ is accompanied by the formation of an oligomeric form of $(RPS)_n$. Evidence for the latter was obtained by monitoring this reaction by ^{31}P NMR spectroscopy (vide infra). Compounds **3b,c** can also be made metathetically from $(MeCp)_2TiCl_2$ and Li_2S_3PR,[23] which is easily prepared in situ from **1b** or **1c** and Li_2S. Compounds **3b,c** were characterized by conventional methods, although NMR spectroscopy proved most useful. The ^1H NMR spectrum of **3b** revealed nonequivalent methyl-

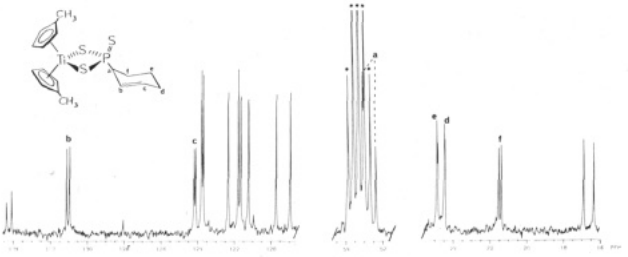

Figure 2. 90.5-MHz $^{13}C\{^1H\}$ NMR spectrum of $(MeCp)_2TiS_3PChe$ (**3c**) in CD_2Cl_2 (asterisk). The 3-cyclohexenyl carbons are indicated by a–f. The eight resonances between 118 and 124 ppm are assigned to the unsubstituted cyclopentadienyl backbone carbons.

cyclopentadienyl groups and the presence of a time-averaged plane of symmetry bisecting the pair of C_5H_4R rings. While the ^1H NMR spectrum of **3c** proved to be uninterpretably complex, its $^{13}C\{^1H\}$ NMR exhibited distinct resonances for each of the 18 nonequivalent carbon atoms in this chiral molecule (Figure 2). The data for **3b** and **3c** are consistent with the $\overline{\text{TiSPS}}$ ring structure (eq 3) but not the valence isomeric phosphorus(III) derivative that would contain a $\overline{\text{TiSSPS}}$ ring.

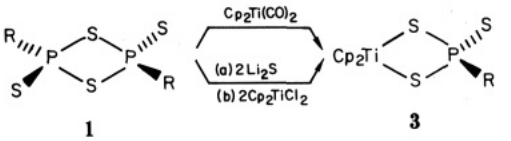

(3)

R = t-Bu, Che

We were able to extend the metathetical synthesis of RPS_3^{2-} chelates to R = An: the complex Cp_2TiS_3PAn (**3a**) is a stable green compound that dissolves in polar organic solvents to give red solutions. Spectroscopic characterization of **3a** revealed that its structure was very similar to **3b** and **3c** which was confirmed by single-crystal X-ray diffraction (vide infra). The ^{31}P NMR chemical shift of **3a** was identical with that which was previously assigned as the "impurity" resonance observed in all ^{31}P NMR spectra obtained from samples of **2a**. Further spectroscopic evidence for the close relationship between the TiS_2P and TiS_2P_2 rings was suggested by the observation that the FDMS of **2a–c** revealed intense peak envelopes at $m/e = M^+ - RPS$.

We have previously employed selenium and sulfur chelates of bis(cyclopentadienyl)titanium as reagents for the preparation of other selenium and sulfur compounds via chelate transfer processes.[4] This methodology applies to **2a** and **3a–c** with an interesting complication. Compound **3a** reacted readily with $NiCl_2$(dppe) to give Cp_2TiCl_2[24] and orange, air-stable $Ni(S_3PAn)$(dppe), **5**. The diamagnetism, color, and spectroscopic properties of the new nickel complex are fully consistent with a square-planar geometry. The same nickel complex formed in excellent yield but much more slowly when $NiCl_2$(dppe) was treated with **2a**. In this case the formation of **5** was accompanied by the formation of $(AnPS)_3$ whose ^{31}P NMR spectroscopic characteristics closely resemble those reported for $(PhPS)_3$[25,26] (eq 4). Compound **5** could also be

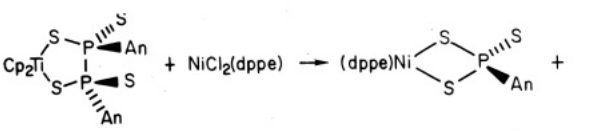

Cp_2TiCl_2 + $\frac{1}{3}(AnPS)_3$ (4)

(22) (a) Harris, R. K. *Can. J. Chem.* **1964**, *24*, 2275. (b) Finer, E. G.; Harris, R. K. *Prog. Nucl. Magn. Reson. Spectrosc.* **1971**, *6*, 61 and references therein. (c) Redfield, D. A.; Cary, L. W.; Nelson, J. H. *Inorg. Chem.* **1975**, *14*, 50 and references therein.

(23) $(NH_4)_2S_3PR$ is one of the products isolated from the reaction of excess NH_3 and $R_2P_2S_4$. Fluck, E.; Binder, H. *Z. Anorg. Allg. Chem.* **1970**, *377*, 298–304.

(24) When monitoring the course of the reaction by ^1H NMR, we observed a resonance at δ 6.40 for Cp_2TiCl_2.

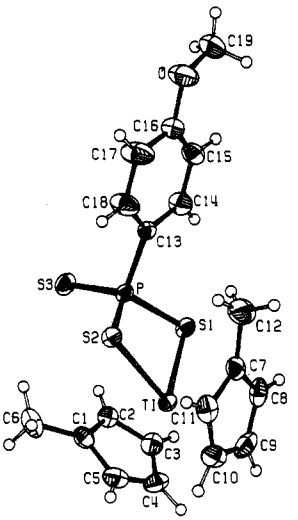

Figure 3. ORTEP view of $(MeCp)_2TiS_3PAn$ showing the labeling scheme for all non-hydrogen atoms. The ellipsoids are drawn with 35% probability boundaries, and the hydrogen atoms are assigned small arbitrary isotropic thermal coefficients.

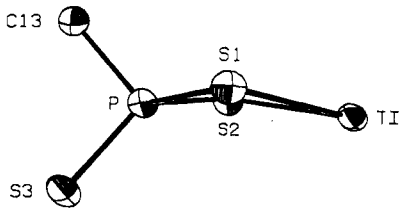

Figure 4. ORTEP drawing of the ring atoms of $(MeCp)_2TiS_3PAn$ viewed normal to the S–S vector showing the large dihedral angle of 167.10°.

prepared from Li_2S_3PAn and $NiCl_2(dppe)$. Compound **5** was further characterized by methylation with CH_3OSO_2F yielding a stable $[Ni(S_2P(SMe)An)(dppe)]^+$, **6**, which was fully characterized as its PF_6^- salt.

Molecular Structure of $(MeCp)_2TiS_3PAn$ (3a). An ORTEP drawing of the molecule is shown in Figure 3. Selected bond distances and angles are given in Table IV.

As predicted from solution spectroscopic data, **3a** consists of $(MeCp)_2Ti$ moiety incorporated into a TiS_2P ring. The parameters associated with the titanium center resemble other $(MeCp)_2TiX_2$ species. The Ti–S distances (2.4898 (8) and 2.4639 (8) Å) are longer than those found in $(Me_5C_5)_2TiS_3$ (2.413 (4) Å).[27] The major difference between TiS_3 and the TiS_2P rings lies in the buckling about the SS vector; in the TiS_3 ring this angle is 131° whereas in **3a**, the angle between the TiS_2 and S_2P planes is 167.10° (Figure 4). The Ti···P distance of 3.099 (2) Å is ~0.6 Å longer than the Ti–S distance whereas the transannular Ti···S distance in Shaver's trisulfide is 2.77 Å. The transannular S···S distances for both compounds are within 0.01 Å of a relatively innocent 3.24 Å (3.2380 (10) Å for **3a** and 3.245 Å for the S_3).

Compound **2a** may be considered to be a close relative of the $(RPS_2)_2$ dimers. A comparison of the structural features of **2a** and $Me_2P_2S_4$ is presented in Table V. The parameters associated with the phosphorus' coordination spheres in these species are closely similar.

(25) (a) Baudler, M.; Koch, D.; Vakratsas, T.; Tolls, E.; Kiper, K. *Z. Anorg. Allg. Chem.* **1975**, *413*, 239–51. (b) LeGeyt, M. R.; Paddock, N. L. *J. Chem. Soc., Chem. Commun.* **1975**, 20.

(26) Lensch, C.; Clegg, W.; Sheldrick, G. M. *J. Chem. Soc., Dalton Trans.* **1984**, 723–5.

(27) Bird, P. H.; McCall, J. M.; Shaver, A.; Siriwardane, V. *Angew. Chem., Int. Ed. Engl.* **1982**, *21*, 384–5.

(28) Daly, J. J. *J. Chem. Soc.* **1964**, 4065–6.

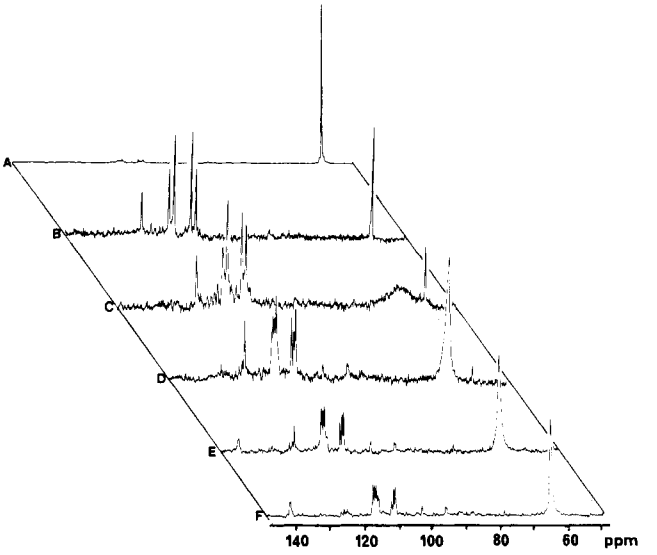

Figure 5. 40.5-MHz $^{31}P\{^1H\}$ NMR spectra for stages in the reaction of $(MeCp)_2Ti(CO)_2$ and **1b**, monitored every 24 h from A–F, respectively. Compound **1b** can be seen in A–D at δ 50.5. Compound **3b** (δ 65.9) can be seen in increasing quantities in spectra C–F. The unsymmetrical intermediate species can be seen in spectra B–E as doublets at δ 117.0 and 111.0 with a phosphorus to phosphorus coupling constant of 49.5 Hz. The oligomeric species $(t\text{-BuPS})_n$ can be seen most clearly in spectrum F as multiplets centered at δ 143, 116, and 110.

Scheme I

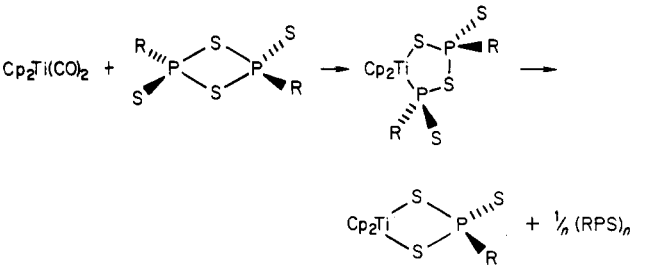

Mechanistic Studies. The key mechanistic issues arising from the synthetic work concern the interrelationships between compounds of the formula $R_2P_2S_4$, $Cp_2TiS_4P_2R_2$, and Cp_2TiS_3PR.

Insight into the formation of **3a** from **1a** was provided by monitoring the relatively slow reaction of $(MeCp)_2Ti(CO)_2$ with **1b** by ^{31}P NMR spectroscopy (Figure 5). The initial product of this reaction is characterized by an AB quartet. This event was followed by the slow formation of a broad resonance for **3b** that sharpened as the concentration of the intermediate diminished. The final spectrum also consists of several features that indicate the presence of an unsymmetrical oligomer of $(t\text{-BuPS})_n$. These observations are consistent with initial formation of an unsymmetrical intermediate followed by the expulsion of an RPS moiety, which subsequently oligomerizes, as shown in Scheme I.

The above experiment suggests a pathway for the interconversion of the $R_2P_2S_4$ and the RPS_3 (R = An) chelates. To further examine this process, the reaction of **3a** with $(PhPS)_3$ was studied by ^{31}P NMR spectroscopy (Figure 6). The reaction is rapid and results in the formation of new resonances that arise from a 1:1:2 mixture of $(MeCp)_2TiS_4P_2An_2$, $(MeCp)_2TiS_4P_2Ph_2$, and $(MeCp)_2TiS_4P_2AnPh$ (AB quartet). The two chemical shifts assigned to $(MeCp)_2TiS_4P_2AnPh$ are similar to those observed for $(MeCp)_2TiS_4P_2Ph_2$ and **2a**. Also present were resonances that correspond to **3a** and one of similar chemical shift that is assigned to the closely related

Table III. Spectroscopic Data

	NMR,[a,b] ppm			FDMS	
	^{1}H	^{31}P{^{1}H}[c]	^{13}C{^{1}H}	*m/e*	assignmt
$(MeCp)_2TiS_4P_2An_2$ **2a**	7.95 (dd, 2 H, J_{PH} = 10.8 Hz)	104.0 (s)		610	M^+
	7.41 (pt, 1 H)			440	$(MeCp)_2TiS_3PAn$
	7.21 (pt, 1 H)				
	6.98 (dd, 2 H, J_{PH} = 3.0 Hz)			408	$(MeCp)_2TiSS_2PAn$
	6.88 (pt, 1 H)				
	6.86 (pt, 1 H)				
	3.84 (s, 3 H)				
	2.14 (s, 3 H)				
$Cp_2TiS_4P_2An_2$ **2b**	7.94 (dd, 2 H, J_{PH} = 10.2 Hz)	108.4 (s)	169.9 (s)	760	$Cp_4Ti_2S_4P_2An_2$
	6.99 (s, 5 H)		134.7 (fid, J_{PC} = 13.1 Hz, J_{PP} = 8 Hz)	582	M^+
	6.88 (dd, 2 H, J_{PH} = 2.8 Hz)		121.0 (s)	567	
	3.84 (s, 3 H)		119.7 (d, J_{PC} = 78 Hz)	445	$CpTiS_4PAn$
			112.8 (fid, J_{PC} = 12.5 Hz, J_{PP} = 8 Hz)	412	Cp_2TiS_3PAn
			55.7 (s)	380	Cp_2TiS_2PAn
$(MeCp)_2TiS_4P_2Pn_2$ **2c**	8.48 (dd, 2 H, J_{PH} = 11.0 Hz)	103.7 (s)		500	$(MeCp)_2TiS_4PPn$
	7.01 (dd, 2 H, J_{PH} = 3.2 Hz)				
	6.65 (m, 2 H)			468	$(MeCp)_2TiS_3PPn$
	6.39 (pt, 1 H)				
	6.05 (pt, 1 H)			436	$(MeCp)_2S_2PPn$
	3.36 (q, 2 H, J_{HH} = 6.9 Hz)				
	1.76 (s, 3 H)			440	M^+
	1.00 (t, 3 H, J_{HH} = 6.9 Hz)				
$(MeCp)_2TiS_3PAn$	8.04 (dd, 2 H, J_{PH} = 15.2 Hz)	33.9 (s)	160.7 (d, J_{PC} = 3.2 Hz)		
	6.98 (dd, 2 H, J_{PH} = 3.0 Hz)		135.3 (s)		
	6.90 (pt, 2 H)		134.6 (s)		
	6.72 (pt, 2 H)		130.6 (d, J_{PC} = 14.5 Hz)		
	6.49 (pt, 2 H)		128.0 (d, J_{PC} = 73.3 Hz)		
	6.45 (pt, 2 H)		124.1 (s)		
	3.86 (s, 3 H)		122.0 (s)		
	2.27 (s, 3 H)		120.4 (s)		
	1.92 (s, 3 H)		119.5 (s)		
			113.0 (d, J_{PC} = 6.0 Hz)		
			55.3 (s)		
$(MeCp)_2TiS_3P$-*t*-Bu **3b**	7.12 (pt, 2 H)	65.9 (s)		390	M^+
	6.60 (m, 4 H)				
	6.48 (pt, 2 H)				
	2.07 (s, 3 H)				
	2.00 (s, 3 H)				
	1.37 (d, 9 H, J_{PH} = 22.3 Hz)				
$(MeCp)_2TiS_3PChe$	7.00 (pt, 2 H)	48.8 (s)	134.3 (s)	414	M^+
	6.69 (dd, 1 H, J_{PH} = 5.1 Hz)		134.0 (s)		
	6.62 (dd, 1 H, J_{PH} = 2.8 Hz)		131.0 (d, J_{PC} = 14.8 Hz)		
	6.53 (pt, 2 H)		124.1 (d, J_{PC} = 7.4 Hz)		
	6.48 (pt, 2 H)		123.7 (s)		
	6.02 (pt, 2 H)		123.6 (s)		
	2.80 (m)		122.3 (s)		
	2.20 (m)		121.7 (s)		
			121.6 (s)		
			121.2 (s)		
			119.7 (s)		
			118.9 (s)		

			52.6 (d, J_{PC} = 59.9 Hz)	
			24.8 (d, J_{PC} = 3.9 Hz)	
			24.4 (d, J_{PC} = 2.0 Hz)	
			21.4 (d, J_{PC} = 8.4 Hz)	
			16.8 (s)	
			16.3 (s)	
Li_2S_3PAn 4	8.11 (dd, 2 H, J_{PH} = 14.0 Hz)	80.0 (s)		
	6.80 (dd, 2 H, J_{PH} = 4.5 Hz)			
	3.82 (s, 3 H)			
$Ni(S_3PAn)(dppe)$ 5	8.20 (dd, 2 H, J_{PH} = 9.0 Hz)	86.6 (t, J_{PP} = 12 Hz)	691	M^+
	7.90–7.62 (m, 10 H)	60.0 (d, J_{PP} = 12 Hz)		
	7.60–7.37 (m, 10 H)			
	6.78 (dd, 2 H, J_{PH} = 3.0 Hz)			
	3.83 (s, 3 H)			
$Ni(S_2P(SMe)An)(dppe)PF_6$ 6	2.31 (d, 4 H, J_{PH} = 17.0 Hz)	97.5 (t, J_{PP} = 8.6 Hz)	705	M^+
	8.0–7.50 (m, 22 H)	65.1 (d, J_{PP} = 8.6 Hz)		
	7.12 (dd, 2 H, J_{PH} = 8.8 Hz)	−145.4 (qn, J_{FP} = 707 Hz)		
	3.90 (s, 3 H)			
	2.68 (m, 4 H)			
	2.59 (d, 3 H, J_{PH} = 16.3 Hz)			

[a] Abbreviations: s (singlet), d (doublet), dd (doublet of doublets), fid (filled in doublet), t (triplet), pt (pseudotriplet), q (quartet), qn (quintet), m (multiplet). [b] All ^1H and ^{13}C NMR obtained in CD_2Cl_2 as solvent except for **4** where $(CD_3)_2CO$ was employed. [c] All data obtained in solvents consisting of a 2:1 ratio of THF-C_6D_6. Compound **6** was run in neat $(CD_3)_2CO$.

Table IV. Selected Bond Distances (Å) and Angles (deg) for $(MeCp)_2TiS_3PAn$

A. Bond Distances

Ti-CpA	2.073 (3)	C13-C14	1.379 (4)
Ti-CpB	2.065 (3)	C14-C15	1.388 (5)
Ti-S1	2.4898 (8)	C15-C16	1.357 (5)
Ti-S2	2.4639 (8)	C16-C17	1.378 (5)
S1-P	2.0624 (10)	C17-C18	1.380 (6)
S2-P	2.0602 (10)	C18-C13	1.375 (4)
S3-P	1.970 (1)	C16-O	1.372 (4)
P-C13	1.814 (3)	O-C19	1.406 (6)

B. Bond Angles

CpA-Ti-CpB	132.1 (1)	S3-P-C13	108.97 (10)
S1-Ti-CpA	107.03 (9)	P-C13-C14	121.5 (2)
S1-Ti-CpB	107.80 (10)	P-C13-C18	120.1 (2)
S2-Ti-CpA	110.01 (9)	C13-C14-C15	121.5 (3)
S2-Ti-CpB	106.7 (1)	C14-C15-C16	119.9 (3)
S1-Ti-S2	81.63 (3)	C15-C16-C17	119.5 (3)
Ti-S1-P	85.27 (3)	C16-C17-C18	120.5 (3)
Ti-S2-P	85.99 (3)	C17-C18-C13	120.9 (4)
S1-P-S2	103.52 (4)	C18-C13-C14	117.7 (3)
S1-P-S3	116.57 (4)	C15-C16-O	124.4 (3)
S2-P-S3	114.72 (4)	C17-C16-O	116.1 (3)
S1-P-C13	105.28 (9)	C16-O-C19	117.9 (3)
S2-P-C13	106.99 (9)		

Table V. Comparison of the Solid-State Structures of $(MeCp)_2TiS_3PAn$ and $(MePS_2)_2$ [a]

bond type	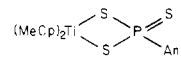	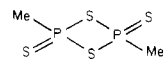
S—P	2.0624 (10)	2.141 (5)
	2.0502 (10)	
S=P	1.970 (1)	1.945 (5)
P—C	1.814 (3)	1.830 (15)
S···S	3.2380 (10)	3.171
Ti···P	3.0992 (8)	2.886 (P···P)
Ti—S—P	85.27 (3)	85.46 (23) (P—S—P)
	85.99 (3)	
S—P—S	103.52 (4)	94.54 (22)
S—P=S	116.57 (4)	116.56 (18)
	114.72 (4)	
S—P—C	105.28 (9)	106.81 (18)
	114.52 (4)	
C—P=S	108.97 (10)	113.54 (51)

[a] See ref 28.

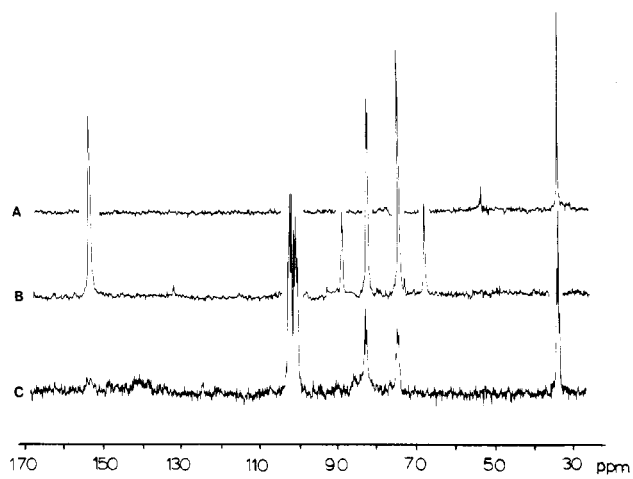

Figure 6. 40.5-MHz $^{31}P\{^1H\}$ NMR spectra of **3a** (A), $(PhPS)_3$ (B), and their reaction mixture taken immediately after dissolution (C), showing the rapid equilibrium between the similar R groups in $(MeCp)_2TiS_4P_2R_2$, $(RPS)_3$, and $(MeCp)_2TiS_3PR$.

$(MeCp)_2TiS_3PPh$. Several sets of broad resonances also occur at chemical shifts centered where those of $(PhPS)_3$ are found. These are interpreted as arising from the eight possible isomers of the unsymmetrical $(RPS)_3$ trimer where

Scheme II

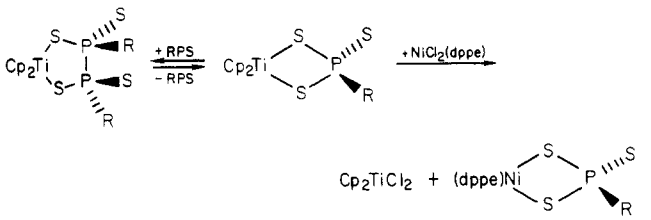

R is An or Ph, indiscriminately combined. This experiment together with the fact that solutions of **2a** invariably contain **3a** clearly establish the facility of the interchange of suitable RPS fragments between **2** and **3**. Taken collectively these results are indicative of an equilibrium as depicted in eq 5. Quantitative ^{31}P NMR spectroscopic

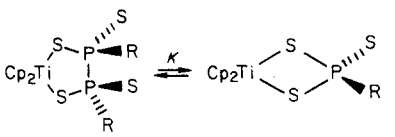

(5)

analysis of solutions of **2a** and **3a** indicated an equilibrium constant of 0.22 (°K) for eq 5. Such an equilibrium also finds support from the relative rates of the reactions of **2a** and **3a** with $NiCl_2$(dppe). The slower rate with which **2a** transfers an RPS_3 chelate is explained by the slow expulsion of an RPS fragment *prior* to RPS_3 chelate transfer (Scheme II).

Discussion

This work introduces two new classes of inorganic heterocycles and provides some insights into their interrelationship. In order to place the new compounds into a more familiar context, we note that the TiS_2P_2 rings found for **2a–c** resemble those found in related dithiolenes[4,29] and $Ph_3P_3S_3$.[25,26]

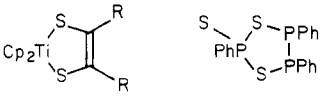

Furthermore, the TiS_2P rings found in compounds **3a–c** can be viewed as hybrids of $Cp_2Ti(PPh)_3$[30,31] and $(C_5Me_5)_2TiS_3$.[27]

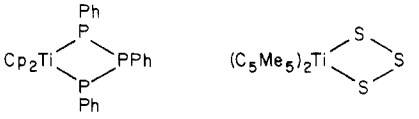

Both the TiS_2P_2 and the TiS_2P cycles are also found in the solid-state polymer TiS_6P_2,[32] a subunit of which is shown.

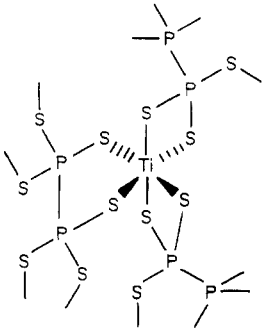

Scheme III

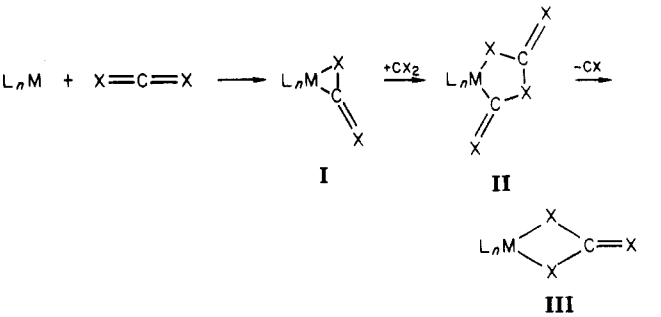

The factors that lend stability to the TiS_2P vs. the TiS_2P_2 cycles are assumed to be steric in accord with the well known effects of substituent size on the stability of rings.[33] The balance between the ring sizes is particularly subtle as shown by the fact that appreciable quantities of **3a** are observed in solutions prepared from pure **2a**. Microscopic reversibility dictates that if RPS *elimination* from the unsymmetrical TiS_2P_2 cycle is facile, as is seen in the reaction of $(MeCp)_2Ti(CO)_2$ with **1b**, the low-energy pathway for *incorporation* of a RPS fragment into **3** (which ultimately produces **2**) must proceed by the reverse process (eq 6). The precise form of the RPS moiety prior to

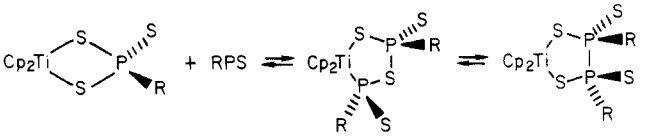

(6)

insertion remains unclear[29] particularly since such compounds exist as dimers or trimers.[25,34] The conversion of the unsymmetrical TiS_2P_2 ring into its symmetrical isomer we propose to occur via an intramolecular pathway involving a phosphorus(III) intermediate (eq 7). Such valence isomerizations have been observed for other organophosphorus compounds,[35] and similar phenomena may be relevant to the mechanism of the isomerization of sulfur rings.[36]

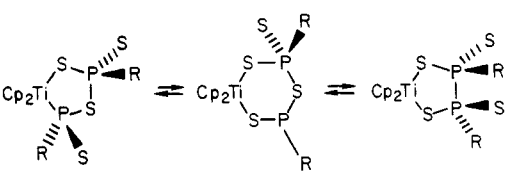

(7)

The interconversion chemistry of these Ti–P–S ring systems is of some relevance to the general patterns for transition metal–heterocumulene reactions. This point is somewhat clearer when one recognizes that the RPS_2 moiety is akin to CS_2 and its congeners. Previous work on the organometallic derivatives of CS_2, COS, and RNCS has established the reaction types shown in Scheme III.[37] There presently exist examples of the conversion of an η^2-CS_2 ligand (type I) to a head-to-tail C_2S_4 type II chelate as in the reaction of $CpRh(C_2H_4)PMe_3$ with CS_2 to give

(29) Villa, A. C.; Manfredolti, A. G.; Guastini, C. *Acta Crystallogr., Sect. B* **1976**, *B32*, 909 and references therein.
(30) Issleib, K.; Wille, G.; Krech, F. *Angew. Chem., Int. Ed. Engl.* **1972**, *11*, 527.
(31) Köpf, H.; Voigtländer, R. *Chem. Ber.* **1981**, *114*, 2731–43.
(32) Jandali, M. Z.; Eulenberger, G.; Hahn, H. *Z. Anorg. Allg. Chem.* **1980**, *470*, 39–44.
(33) Shaw, B. L. *J. Am. Chem. Soc.* **1975**, *97*, 3856–7.
(34) Cetinkaya, B.; Hitchcock, P. B.; Lappert, M. F.; Thorne, A. J.; Harold, G. *J. Chem. Soc., Chem. Commun.* **1982**, 691–3.
(35) Lindner, E.; Dreher, H. *Angew. Chem., Int. Ed. Engl.* **1975**, *14*, 416–7.
(36) Steudel, R. *Top. Curr. Chem.* **1982**, *102*, 149–76.
(37) Ibers, J. A. *J. Chem. Soc. Rev.* **1982**, *11*, 57–73 and references therein.

Scheme IV

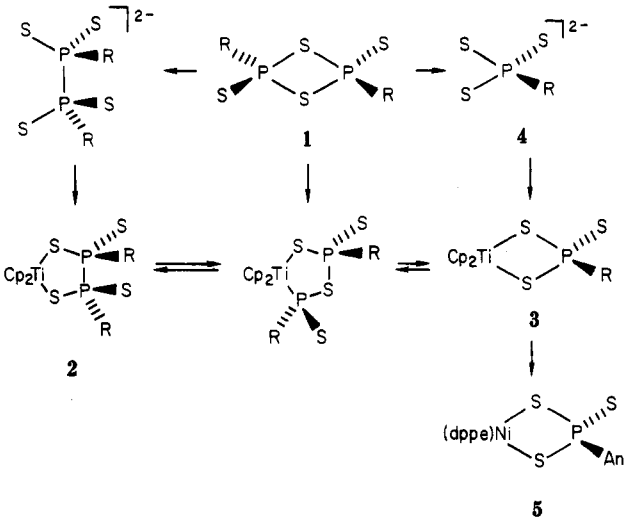

$CpRhC_2S_4(PMe_3)$ as reported by Werner.[38] Gafney and Ibers have shown that a similar type I ligand in $Ru(CO)_2(PPh_3)_2(\eta^2\text{-COS})$ reacts with an excess of COS to yield a type III chelate, $Ru(CO)_2(PPh_3)_2(S_2CO)$.[39] The results presented in this paper provide examples of the facile interconversions of a type II to a type III chelate, by the expulsion of an RPS moiety from a type II chelate. Most likely the insertion of PhPS into the type III chelate **3a** is an example of the conversion of a head-to-tail type II chelate into its symmetrical head-to-head isomer, **2a**. Head-to-head couplings of heterocumulenes have only previously been observed for bimetallic systems.[40,41] These results are summarized in Scheme IV.

Acknowledgment. This research was supported by the National Science Foundation (CHE-81-06781), and we also thank the donors to the Petroleum Research Fund, administered by the American Chemical Society. We thank Dr. S. R. Wilson for his assistance with the crystallography. Dr. Mark Draganjac was helpful in working up the crystallographic data. High-field NMR spectra were obtained through the NSF Midwest Regional NMR center (CHE 79-16100).

Registry No. **1a**, 90412-95-6; **1b**, 90412-96-7; **1c**, 90412-97-8; **2a**, 90432-13-6; **2b**, 90412-98-9; **2c**, 90412-99-0; **3a**, 90413-00-6; **3b**, 90413-01-7; **3c**, 90432-14-7; **4**, 90412-94-5; **5**, 90413-02-8; **6**, 90413-04-0; $Cp_2Ti(CO)_2$, 12129-51-0; Cp_2TiCl_2, 1271-19-8; $(MeCp)_2TiCl_2$, 1271-19-8; $(MeCp)_2Ti(CO)_2$, 90413-05-1.

Supplementary Material Available: Tables of thermal parameters and all hydrogen atom parameters of **3a** and structure factors (16 pages). Ordering information is given on any current masthead page.

(38) Werner, H.; Kolb, O.; Feser, R. *J. Organomet. Chem.* **1980**, *191*, 283–93.
(39) Gaffney, T. R.; Ibers, J. A. *Inorg. Chem.* **1982**, *21*, 2860–4.
(40) Maj, J. J.; Rae, A. D.; Dahl, L. F. *J. Am. Chem. Soc.* **1982**, *104*, 4278–80.
(41) Fachinetti, G.; Biran, C.; Floriani, C.; Chiesi-Villa, A.; Guastini, C. *J. Am. Chem. Soc.* **1978**, *100*, 1921–2.

Reactions of Crowded Secondary Phosphines with $(\eta^3\text{-2-XC}_3H_4)M(1,5\text{-COD})$ (X = H or Me and M = Rh or Ir)

Brendan D. Murray and Philip P. Power*

Department of Chemistry, University of California, Davis, California 95616

Received February 13, 1984

A series of rhodium(I) and iridium(I) phosphine complexes have been prepared by treating $(\eta^3\text{-2-XC}_3H_4)M(\eta^4\text{-1,5-COD})$ (where X = H or Me and M = Rh or Ir) with di-*tert*-butylphosphine, dicyclohexylphosphine, and bis[bis(trimethylsilyl)methyl]phosphine. Intermediates have been isolated that involve various degrees of substitution by the phosphines as well as the product of an unusual rearrangement involving the $PH\{CH(SiMe_3)_2\}_2$ ligand. ^{31}P and ^1H NMR, GC/MS, and X-ray methods were used to identify the products of these reactions. Many of the complexes react with hydrogen and readily hydrogenate simple olefins. The molecular structures of $(\eta^3\text{-2-MeC}_3H_4)Rh[PH(C_6H_{11})_2]_2$, **2**, $(\eta^4\text{-1,5-COD})Rh(\eta^3\text{-2-MeC}_3H_4)[PH(t\text{-Bu})_2]$, **3**, and $(\eta^4\text{-1,5-COD})Ir(\eta^3\text{-2-MeC}_3H_4)[PH(t\text{-Bu})_2]$, **5**, have been determined by X-ray diffraction. The crystal data at 140 K are as follows. **2**: a = 10.637 (2) Å, b = 12.242 (2) Å, c = 12.453 (3) Å, α = 104.88 (2)°, β = 94.962 (2)°, γ = 111.57 (2)°, Z = 2, space group $P1$ (No. 2). **3**: a = 9.130 (2) Å, b = 9.821 (3) Å, c = 12.262 (4) Å, α = 105.13 (3)°, β = 99.34 (2)°, γ = 105.70 (3)°, Z = 2, space group $P1$. **5**: a = 9.151 (2) Å, b = 9.778 (2) Å, c = 12.304 (3) Å, α = 104.77 (2)°, β = 99.34 (2)°, γ = 106.05 (1)°, Z = 2, space group $P1$. Complex **2** is essentially square planar. Complexes **3** and **5** are both square pyramidal with the phosphine occupying the axial position. In **3** the Rh–P distance is 2.457 (1) Å while the Ir–P distance in **5** is 2.402 (3) Å. These distances are much greater than the values reported for similar structures containing smaller phosphines and phosphites as the axial ligand.

Introduction

The reactions of $[(\eta^4\text{-1,5-COD})Rh(\eta^3\text{-2-XC}_3H_4)]$ (where X = H or Me) with various types of phosphines and phosphites have been examined in a number of recent publications.[1-4] The addition of small phosphorus ligand(s) has resulted in the loss of the COD group to produce some interesting four- and five-coordinate complexes. These complexes characteristically have the phosphorus ligands arranged in a cis geometry.

(1) Murray, B. D.; Olmstead, M. M.; Power, P. P. *Organometallics* **1983**, *2*, 1700.
(2) Fryzuk, M. D. *Inorg. Chem.* **1982**, *21*, 2134.
(3) Fryzuk, M. D. *Inorg. Chim. Acta* **1981**, *54*, L265.
(4) Sivak, A. J.; Muetterties, E. L. *J. Am. Chem. Soc.* **1979**, *101*, 4878.

0276-7333/84/2303-1199$01.50/0